

1 **Probing bacterial-fungal interactions at the single cell level**

2
3 ¹Claire E. Stanley*, ²Martina Stöckli*, ¹Dirk van Swaay, ³Jerica Sabotič, ²Pauli T. Kallio, ²Markus Künzler,

4 ¹Andrew J. deMello°, ²Markus Aebi°

5
6 ¹Institute for Chemical and Bioengineering, Department of Chemistry and Applied Biosciences, ETH Zürich, Vladimir-
7 Prelog-Weg 1, CH-8093 Zürich, Switzerland

8
9 ²Institute of Microbiology, Department of Biology, ETH Zürich, Vladimir-Prelog-Weg 4, CH-8093 Zürich, Switzerland

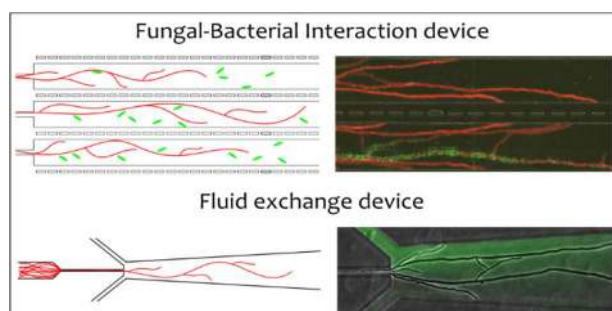
10
11 ³Department of Biotechnology, Jožef Stefan Institute, Jamova 39, SI-1000 Ljubljana, Slovenia

12
13
14 * These authors contributed equally to this work

15
16 ° Corresponding authors

17
18 **Table of Content Entry**

19 We detail two microfluidic platforms that enable the *dynamic* interactions between filamentous fungi and bacteria
20 to be monitored at the single cell level and in real-time.



21
22
23 **Abstract**

24 Interactions between fungi and prokaryotes are abundant in many ecological systems. A wide variety of
25 biomolecules regulate such interactions and many of them have found medicinal or biotechnological applications.
26 However, studying a fungal-bacterial system at a cellular level is technically challenging. New microfluidic devices

27 provided a platform for microscopic studies and for long-term, time-lapse experiments. Application of these novel
28 tools revealed insights into in the dynamic interactions between the basidiomycete *Coprinopsis cinerea* and *Bacillus*
29 *subtilis*. Direct contact was mediated by polar attachment of bacteria to only a subset of fungal hyphae suggesting a
30 differential competence of fungal hyphae and thus differentiation of hyphae within a mycelium. The fungicidal
31 activity of *Bacillus subtilis* was monitored at a cellular level and showed a novel mode of action on fungal hyphae.

32

33 **Keywords:** Bacterial-fungal interaction (BFI) / microfluidics / antifungal mode of action / single cell microscopy

34

35 **Insight, innovation, integration**

36 The integration of microfluidic platforms with a growing filamentous mycelium and bacteria opens a great potential
37 for interaction analysis. Currently, no method exists that enables the *dynamic* interactions between filamentous
38 fungi and bacteria to be monitored at the single cell level and in real-time. The confinement provided by the
39 bacterial-fungal interaction device enables the spatiotemporal fingerprints of bacterial-fungal associations to be
40 assessed. In contrast, our exchange device enables the fluidic environment surrounding hyphae to be manipulated.
41 Together, these devices provide a novel means to assess and dissect these complex relationships at the single cell
42 level and have revealed novel insights into the interaction of *B. subtilis* with *C. cinerea*, such as bacteria-induced
43 blebbing of hyphal cells and dynamic polar attachment.

44

45 **Introduction**

46 Bacteria and fungi often share the same habitat and their interactions can have major implications on the biology of
47 the partners involved and on the respective environment.¹⁻⁵ These microorganisms are found closely associated in
48 environmental samples with bacteria attaching to fungal hyphae.⁶ Dung of herbivorous animals, as an example, is a
49 nutrient-rich environment where bacteria and fungi interact and compete for resources.⁷ Fungi and bacteria share a
50 lifestyle of nutrition by absorption and thus antagonistic strategies have evolved in both clades due to this trophic
51 competition.⁸ From such strategies, important applications in the medical and agricultural sciences have emerged;
52 for example, antibacterial secondary metabolites and peptides from fungi are used as antibiotics⁹⁻¹¹ and different
53 bacterial species are studied as biological control agents in agriculture against plant pathogenic fungi.¹²⁻¹⁵ Due to
54 technical limitations, dynamic bacterial-fungal interactions at the single cell level are not well studied. As such, there
55 is a need for the development of new technological platforms to interrogate and quantify these complex and
56 dynamic interactions, presenting opportunities to gain insights into the phenotypic heterogeneities and spatial
57 organisations of mixed microbial communities, for example.

58
59 Traditional approaches for exploring interactions between fungi and bacteria are based on confrontation assays,
60 where axenic fungal and bacterial inocula are introduced onto solid or into liquid media, incubated together for a
61 period of time and the growth of the interacting species measured.^{13, 16} These assays monitor bacterial-fungal
62 interactions (BFIs) at the macroscopic level, e.g. by growth inhibitions. However, such measurements yield limited
63 information at the cellular level, since specific interactions between hyphae and bacteria and their spatial
64 organisation cannot easily be monitored. Assays using multi well-plates¹⁴ provide one approach for obtaining
65 information at the microscopic level. However, high-resolution imaging, hyphal tracking and media exchange are
66 challenging in such a setup. Conventional microscopic imaging, where hyphae are grown on microscopy slides
67 coated with agar,¹⁷ for example, are also subject to similar drawbacks, particularly in the sense that it is difficult to
68 monitor dynamic interactions in real time due to a lack of confinement. Currently, there are few tools that allow the
69 control of environmental conditions in a precise and dynamic manner and at the same time, the monitoring of
70 interactions at a microscopic level.

71
72 Microfluidics describes the use of engineered systems, possessing micron-scale features, to control, manipulate and
73 analyse pL- μ L fluid volumes.¹⁸ Originally developed for use in the chemical sciences, microfluidic devices have been
74 shown to provide for enhanced analytical performance,¹⁹ high-throughput experimentation²⁰ and controlled

75 generation of chemical gradients,²¹ for example. In recent years, the use of microfluidic systems in the
76 microbiological sciences has grown apace, owing to the ease in manipulating microorganisms on a single cell basis
77 and the ability to control microenvironments in a rapid and precise manner.²² Importantly, the use of
78 microfabrication techniques for the rapid and inexpensive production of microfluidic devices allows bespoke
79 systems to be designed for the problem at hand, unlocking new experimental opportunities for microbiologists. The
80 polymer, poly(dimethylsiloxane) (PDMS), is an ideal substrate material for use in biological applications, having
81 desirable physical and chemical properties.²³ Importantly, this elastomeric polymer is permeable to gases, enabling
82 experiments to be conducted in an aerobic environment, and allows optical detection from 240 – 1100 nm.²⁴

83
84 Methods currently available for processing live microorganisms-on-a-chip are most frequented by technologies that
85 explore bacterial microenvironments. As summarised by Wessel *et al.*,²⁵ the main advantages afforded by these
86 studies include the ability to confine cells, where the influence of spatial structure on the behaviour of bacterial cells
87 can be examined,²⁶ and detect small-molecules, leading to a better understanding of the composition and variation
88 in the microenvironment.²⁷ As a result, light has been shed on a variety of topics including bacterial chemotaxis,²⁸
89 phenotypic heterogeneity in populations of bacteria²⁹ and quorum sensing.³⁰ Studies utilising filamentous fungi in
90 microfluidic devices have emerged only very recently, with a clear focus on probing the growth dynamics of
91 filamentous fungi using microfabricated structures.³¹ Microfluidic technologies entertaining mixed microbial
92 populations, such as the microfluidic droplet platform described by Park *et al.*³² for detecting symbiotic relationships
93 in communities comprised of multiple populations of bacteria, are rare and, at present, no method exists that
94 enables dynamic interactions between bacteria and filamentous fungi to be monitored using microfluidic platforms
95 at the cellular level and quantified in real-time. Further, it is not possible to exchange media surrounding hyphae and
96 monitor their response in a controlled manner using conventional methods; such a feat would add a significant new
97 dimension to the mycological toolbox.

98
99 To address the aforementioned needs, we present a novel microfluidic platform that enabled bacterial-fungal
100 interactions to be probed and fluid exchange to be performed in a controlled and rapid manner. The first
101 microfluidic device allows confrontations between the bacteria and fungi in a confined environment. A key feature
102 of this device, when compared to macroscale systems, is the confinement of submerged hyphae (defined by the
103 height of the microchannel) to a single layer. In turn, this allows the same hyphae or hyphal compartment to be
104 monitored over extended periods of time using high-resolution optical microscopy. Furthermore, bacteria can freely

105 move within the system and physical interactions between bacteria and hyphae can be studied with high spatial and
106 temporal resolution. The second device enables complete exchange of the medium surrounding hyphae in less than
107 4 minutes, where the amount of compound required for such experiments is low. Thanks to the fast fluidic
108 exchange, we are able to determine the time required for hyphae to respond to a stimulus. To demonstrate the
109 efficacy of our approach, both microfluidic platforms are used to study the interaction of the coprophilous
110 basidiomycete, *Coprinopsis cinerea* (*C. cinerea*), with the soil dwelling bacterium *Bacillus subtilis* (*B. subtilis*). *C.*
111 *cinerea* hyphae secrete antibacterial peptides that are active against gram-positive bacteria such as *B. subtilis*,³³ whilst
112 *B. subtilis* exhibit antifungal activity,³⁴ providing an interesting BFI. Our new analytical technology provides novel and
113 surprising insights into the fungal lifestyle and the “mode of action” of BFIs at a cellular level.

114

115 **Results and discussion**

116

117 **Device structure**

118 The two devices detailed herein were fabricated using a structured PDMS top layer, containing micron-sized features
119 and a glass-bottomed petri dish as the bottom layer. Upon sealing the two layers together, following oxygen plasma
120 treatment, microchannels were filled immediately with the medium of choice. *C. cinerea* was grown on YMG for
121 three days at 28°C and a fungal inoculum, taken from the peripheral growth zone, was placed next to the opening of
122 the microchannels, as illustrated in Figure 1a. The entire device was incubated in a dark, humid environment for 18
123 hours, under constant temperature (28°C), during which time hyphae grow and enter the microchannels. An agar
124 plug containing the fungal mycelium was used to introduce hyphae into the device; however, it is important to note
125 that the device design can easily be adapted to allow incorporation and germination of individual fungal spores.

126

127 The first device design, which we term the bacterial-fungal interaction (BFI) device, is detailed in Figure 1 and
128 provides an environment whereby bacteria can interact with hyphae of *C. cinerea*. Device operation is detailed fully
129 in Supplementary Method 1. The key components of this device include: i) 28 microchannels arranged in parallel,
130 where hyphae are confined in the z-direction, ii) a constriction point, which limits and controls the number of
131 hyphae entering each microchannel and iii) an inlet, where bacteria are introduced into the system. Each hyphal
132 observation channel is 110 µm in width, nearly 7 mm in length and 10 µm in depth, with a constriction width of 20
133 µm. A channel depth of 10 µm was chosen, primarily to confine *C. cinerea* hyphae (which have a diameter of
134 approximately 7 µm) but also to provide sufficient room for bacteria to interact with the hyphae. The bacterium, *B.*

135 *subtilis*, has a length on the order of 1 μm and can therefore navigate around the hyphae within a microchannel. The
136 long, narrow microchannels permit long-term time-lapse imaging to be conducted, allowing hyphal growth to be
137 monitored for up to 24 h. Figure 1e shows a leading hypha growing in a microchannel at an average rate of 4.2 ± 1.0
138 $\mu\text{m}/\text{min}$; we determined a branch growth rate of $2.1 \pm 0.2 \mu\text{m}/\text{min}$. Further, clamp cell and septa formation were
139 observed (see Supplementary Movie 1 and 2). As the microchannel dimensions act to confine the length of a single
140 hypha, as well as subsequent branching events, the volume directly surrounding each hypha is limited. Hence, an
141 environment, whereby bacteria can be confined in the vicinity of each hypha, is afforded and dynamic interactions
142 between bacteria and hyphae may be monitored. To introduce bacteria and to allow interaction with hyphae, 10 μL
143 of a bacterial suspension (containing bacteria in CCMM with an optical density at 600 nm of 1) was pipetted into the
144 device inlet. As *B. subtilis* is a motile bacterium, it is able to explore its environment and interact with the fungal
145 hyphae independently, as illustrated in Supplementary Movie 3. Moreover, as this is a closed system, the spatial
146 distribution of the bacteria relative to the hyphae and their dynamic interactions could be monitored in real time,
147 without dilution.

148

149 The ability to access and manipulate the fluid surrounding the hyphae is a desirable function. As this cannot be
150 achieved in a direct way using the BFI device, a second device was designed for this specific purpose and is termed
151 the fluid exchange device. Figure 2a-c illustrate a three-dimensional representation of the device design and the
152 mask design respectively (operation is described in Supplementary Method 1).

153

154 The fluid exchange device acts to passively pump fluid into the main observation channel and possesses a
155 constriction channel, a tapered observation channel, an inlet and an outlet. The constriction channel was designed
156 to be 10 μm in both width and height, with a length of 400 μm , thus limiting the number of hyphae entering the
157 observation channel. More importantly, the hyphae are exploited as a means to block the constriction junction,
158 providing a region of high fluidic resistance, which diverts the flow to the outlet via a tapered observation channel.
159 This channel creates a zone of lower fluidic resistance in the direction of the outlet. As such, there is minimal
160 interaction of the substance of interest with the rest of the mycelium. It was found that the ideal location of the
161 delivery channels (which transfer material from the inlet to the main observation channel) is situated at the
162 beginning of the tapered observation channel. When a hypha first passes through the constriction channel and
163 enters into the tapered channel, it grows in a polarised manner towards the outlet. Hyphal tips are often observed
164 tracking the edge of the microchannel (see Supplementary Movie 4) and branching events occur at angles between

165 70 and 75 degrees³⁵ relative to the main hyphal body (in the direction of the tip). Accordingly, the placement of the
166 delivery channels at the beginning of the tapered observation channel opposes the natural polarised growth of
167 hyphae, minimizing any blockage of channels due to fungal growth.

168
169 To demonstrate operation, *C. cinerea* minimal medium (CCMM) was exchanged with an aqueous, fluorescein-
170 containing solution. It was found that fluid exchange occurs in less than 4 minutes (Figure 2d and Supplementary
171 Figure S1) and 100 % exchange of the fluid achieved when washing steps were incorporated into the exchange
172 process (see Supplementary Method 2 and Figure S2). Figure 2e illustrates complete removal of a fluorescein
173 solution from the main observation channel, when exchanged with CCMM. Importantly, control experiments, where
174 CCMM was exchanged with CCMM, do not result in an arrest of hyphal growth. To summarize, the advantages
175 associated with the fluid exchange device include the ability to exchange or collect media directly surrounding
176 hyphae and the ability to introduce both, motile and non-motile, bacteria accordingly. The fluid exchange device
177 opens up new avenues, where hyphae can be interrogated with specific biochemical agents and the response
178 monitored in real time. In addition, live/dead assays can be conducted and the chemical and biological species
179 expressed by the fungus in the presence of different bacteria (and vice versa) can be analysed directly.

181 **Interaction between *C. cinerea* and *B. subtilis* in the BFI device**

182 We applied the microfluidic device to monitor the interaction of *C. cinerea* with *B. subtilis*. Different *Bacillus* species
183 produce biologically active lipopeptides from the surfactin, iturin and fengycin families,³⁴ with many of these
184 lipopeptides showing antifungal properties. The confrontation of *C. cinerea* strain AmutBmut with two different
185 strains of *B. subtilis*, the laboratory strain, *B. subtilis* 168, and the wild-strain, *B. subtilis* NCIB 3610,³⁶ was initially
186 performed on a CCMM agar plate as a classical confrontation assay (Figure 3a). Growth inhibition of *C. cinerea* was
187 observed only in the presence of *B. subtilis* NCIB 3610, as indicated by clear exclusion zones. Previous studies have
188 demonstrated that this *B. subtilis* strain produces antifungal agents that inhibit the growth of different plant
189 pathogenic oomycetes and ascomycetes,³⁷ whereas the laboratory strain, *B. subtilis* 168, does not produce any of
190 the antifungal lipopeptides.³⁸ The confrontation assay defined the growth inhibitory action of *B. subtilis* NCIB 3610 at
191 a macroscopic level and without direct contact, but revealed little information regarding the mode of interaction
192 between the two organisms. Accordingly, we used the BFI device to monitor the physical interaction of bacteria with
193 hyphae over time. Upon addition of the two *B. subtilis* strains into the microfluidic system, attachment of bacteria to
194 the hyphae in an end-on manner was observed (Figure 3b and c), suggesting that the bacterial binding site was

195 exposed at the bacterial cell pole. To visualize the attachment pattern, *C. cinerea* strain AmutBmut pMA412,
196 expressing the cytoplasmic fluorescent dTomato protein under the control of the constitutive *Agaricus bisporus*
197 *gpdII* promoter,³⁹ and *B. subtilis* pMF37, expressing the green-fluorescent protein under the control of the
198 constitutive hyper *spac* promoter integrated into the *amyE* locus,⁴⁰ were introduced into the BFI device.
199 Interestingly, bacteria attached only to certain hyphae (Figure 4) and no attachment to the newly formed surface of
200 growing hyphae was detected: a zone extending from the growing hyphal tip was free of attaching bacteria. This
201 attachment pattern was identical for both bacterial strains, suggesting that some hyphae were competent for
202 bacterial attachment while others were not. However, the binding site on the competent hyphae is unknown.
203 Bacteria killed using ultraviolet illuminations (see Supplementary Method 3) and introduced subsequently to *C.*
204 *cinerea* hyphae also attached to the hyphae in the same way. We concluded that hyphal differentiation and
205 competence for attachment was present prior to hyphae and bacteria coming into contact. Our results provided
206 direct evidence for functional differentiation of living hyphae within the mycelium. This differentiation has also been
207 proposed recently by Wösten and co-workers, where differential transcriptional and translational activity⁴¹ and RNA
208 composition in an *Aspergillus niger* mycelium was reported.⁴² Differential attachment has also been described for
209 the interaction between *Pseudomonas aeruginosa* and *Candida albicans* hyphae, but only for single hyphae and not
210 within the same mycelium.⁴³ Toljander *et al.* showed that bacterial attachment differed for living and dead hyphae.⁴⁴
211
212 Furthermore, bacterial attachment to hyphae and the local concentration of free bacteria was found to change over
213 time, as illustrated in Figure 4. Bacterial attachment to hyphae decreased after a high local concentration of free
214 bacteria resided in the vicinity (see Figure 4). Supplementary movies 5 and 6 demonstrate regions containing a high
215 local concentration of *B. subtilis* NCIB 3610 in close proximity to hyphae. Interestingly, these bacterial associations
216 moved along the microchannels in clusters, suggesting a coordinated behaviour of the bacteria. Attachment of
217 bacteria to hyphal cells has been described before⁴³⁻⁴⁷ with some bacteria initially attaching in an end-on manner to
218 the hyphae.^{48, 49} However, the dynamics of the attachment could not be determined with the methods previously
219 used. Using our BFI device it was observed that the attachment and local bacterial concentration change over time.
220
221 We used the same experimental platform to study the long-term growth characteristics of *C. cinerea* leading hyphae
222 in the presence and absence of the two *B. subtilis* strains. *C. cinerea* hyphae were allowed to grow into the BFI
223 device until they reached the observation channels thereby plugging the constriction. Such plugging did not prevent
224 fungal growth in the observation channel. Subsequently, bacteria were introduced into the microchannels via the

225 inlet and a time-lapse (30 minute time interval) over the whole length of seven microchannels conducted. Using the
226 same setup, a control experiment was performed in the absence of bacteria. The growth rate of the leading hyphae
227 in the control experiment was $6.2 \pm 1.4 \mu\text{m}/\text{min}$ and $5.0 \pm 1.5 \mu\text{m}/\text{min}$ in the presence of the laboratory strain, *B.*
228 *subtilis* 168 (Figure 5a). Upon introduction of the wild-strain, *B. subtilis* NCIB 3610, into the BFI device, the growth
229 rate of the leading hyphae was initially comparable, having a growth rate of $5.3 \pm 1.2 \mu\text{m}/\text{min}$ during the first five
230 hours of the experiment. After this time, however, leading hyphae stopped growing (Figure 5a) with a change of the
231 morphology of some fungal apical cells, becoming transparent and thinner in nature (Figure 5b, arrows). A clear
232 difference in morphology between affected hyphal cells and adjacent cells was observed. Interestingly, branches
233 growing from hyphal cells distal to affected cells continued to propagate, indicating the functionality of the adjoining
234 cells. Importantly, the morphological changes described were not observed for the experiments involving *B. subtilis*
235 strain 168.

236
237 To visualize the cellular response of hyphae interacting with *B. subtilis* more precisely, the fluorescent *C. cinerea*
238 strain AmutBmut pMA412 was introduced into the BFI device and co-inoculated with bacteria using the same
239 experimental approach as described above. Figure 6a details a series of images taken over a period of 8 hours and
240 20 minutes and illustrates the morphological change that was described above of several cells. These cells resemble
241 collapsed hyphal compartments, with a loss of dTomato fluorescence. Simultaneously, we observed blebs containing
242 fluorescent dTomato emerging from these hyphal compartments (Figure 6a, b and Supplementary Movie 7), most
243 likely the cause for the loss of cellular content in these cells. Some of the blebs were stable for up to several hours.
244 The confined location of extracellular dTomato fluorescence suggests that these blebs consisted of membranes
245 encompassing the cytoplasmic content. This process takes place mainly in apical cells and, interestingly, did not
246 show any correlation with the attachment of bacteria to the hyphae. Figure 6b exemplifies a collapsed hyphal
247 compartment; two adjoining cells were still intact five hours after addition of the *B. subtilis* wild-strain, however, one
248 of these hyphal compartments had collapsed within the next 30 minutes. The distal cell remained intact, indicating
249 that the dolipore was closed. These experiments demonstrated that *B. subtilis* NCIB 3610 was capable of arresting
250 growth of the leading hyphae by inducing collapse of some of the hyphal compartments. Interestingly, bacterial
251 attachment did not correlate with the collapse of hyphal compartments. Contrarily, attachment of *P. aeruginosa* to
252 *C. albicans* hyphae leads to the establishment of biofilms and is important for the subsequent contact mediated
253 killing of hyphae.^{43, 49}

254

255 **Effect of *B. subtilis* cell-free supernatant on *C. cinerea* hyphae**

256 To elucidate if the direct interaction of bacteria with hyphae was required for the fungicidal effect observed, *B.*
257 *subtilis* cell-free supernatant (see Supplementary Method 4) was tested on *C. cinerea* pMA412 hyphae. The two *B.*
258 *subtilis* strains were sub-cultured in CCMM for 20 hours in the absence of *C. cinerea*. Bacteria were removed by
259 centrifugation and sterile-filtered supernatant was added to *C. cinerea* hyphae using the fluid exchange device. After
260 exchange of CCMM with the *B. subtilis* NCIB 3610 conditioned medium, hyphal apical cells collapsed in a fashion
261 comparable to that observed in the presence of bacteria – that is, with the occurrence of blebs (Figure 6a and b and
262 Supplementary Movie 8). Moreover, it was apparent that the shape of the hyphal tip changed first, a few minutes
263 after application of the conditioned medium. Blebbing was observed only for some apical cells, but all hyphae
264 stopped growing after addition of the conditioned medium from *B. subtilis* NCIB 3610. As expected, this did not
265 occur when the medium surrounding the hyphae was exchanged with *B. subtilis* 168 conditioned medium
266 (Supplementary Figure S3).

267

268 It is well known that some *Bacillus* lipopeptides harbour antifungal effects, especially lipopeptides from the iturin
269 and fengycin family which are active against filamentous fungi.^{13, 14, 50-53} Both *B. subtilis* strains contain non-ribosomal
270 peptide synthase (NRPS) gene clusters to produce the lipopeptides surfactin and fengycin. Due to a mutation in *sfp*,
271 whose gene product is required for the activation of both NRPSs, *B. subtilis* 168 does not produce these
272 lipopeptides.^{54, 55} Therefore, we assessed whether lipopeptides were responsible for the blebbing phenotype. Taking
273 advantage of the fact that lipopeptides are *n*-butanol extractable and thermostable,^{14, 50} we extracted components
274 from conditioned medium with *n*-butanol, evaporated it to dryness and resuspended the dried film in CCMM. The
275 morphological changes of *C. cinerea* hyphae, upon addition of this solution, were monitored in the exchanging
276 device. Additionally, we heat treated the conditioned medium for 15 min at 100°C. Both treatments did not abolish
277 the formation of blebs nor the collapse of apical cells (see Supplementary Table S1). To exclude any effect due to
278 remaining *n*-butanol, the medium was exchanged with CCMM containing 1 % (v/v) *n*-butanol. No growth stop or
279 collapse of apical cells was observed. These experiments suggest that growth arrest and the formation of blebs were
280 both elucidated by *n*-butanol extractable activities and not by enzymes produced by the bacteria. Importantly, this
281 activity affected cell wall properties and not plasma membrane permeability, because cytoplasm-containing blebs
282 were observed. A similar observation was also reported for the *Bacillus amyloliquefaciens* action on *Fusarium*
283 *oxysporum* hyphae.⁵⁶ These experiments also demonstrate different modes of experimentation that become
284 possible using the fluid exchange device.

285 **Experimental**

286

287 **Strains and cultivation conditions**

288 Fungal and bacterial strains used in this study are summarised in Supplementary Table S2. *Escherichia coli* DH5 α was
289 used for cloning and maintenance of plasmids. Preparation of transformation competent cells was carried out as
290 described by Inoue *et al.*⁵⁷ *E. coli* DH5 α containing pMF37 and pRS426 plasmids and its derivatives was selected on
291 Luria-Bertani (LB) medium containing 100 μ g/mL ampicillin (see Supplementary Materials). *Saccharomyces*
292 *cerevisiae* laboratory strain W303a (*MATa ade2-1 leu2-3,112 his3 ura3-1 can1-100 trp1-1*) was used for homologous
293 recombination of plasmids and was maintained on Yeast extract-Peptone-Dextrose (YPD) medium (see
294 Supplementary Materials) at 30°C and transformants were selected on synthetic complete dextrose without uracil
295 (SD Ura-) agar plates.⁵⁸ The laboratory strain, *B. subtilis* 168, and the wild-strain, *B. subtilis* NCIB 3610, were
296 maintained on LB medium, the *B. subtilis* strains containing inserted pMF37 plasmids on LB medium with 100 μ g/mL
297 spectinomycin. *E. coli* and *B. subtilis* strains were grown aerobically at 37°C if not otherwise stated. *C. cinerea* strain
298 AmutBmut⁵⁹ was cultivated on solid yeast-malt extract-glucose (YMG) medium (see Supplementary Materials) at
299 28°C in a dark and humid environment.

300

301 **Plasmids**

302 Plasmids and primer used in this study are listed in Supplementary Table S3 and S4, respectively. Cloning by
303 homologous recombination was carried out in *S. cerevisiae* W303a as described previously.⁵⁸ Construction of plasmid
304 pMA412 is described in Supplementary Method 5. Plasmids were transformed into *C. cinerea* strain AmutBmut by
305 protoplasting of the mononucleate asexual spores (oidia) as described previously.⁶⁰ Plasmid pMF37 was integrated
306 into the *amyE* locus on the chromosome by homologous recombination. The plasmid was introduced into *B. subtilis*
307 cells by natural competence.⁶¹

308

309 **Confrontation assay on agar plates**

310 An agar plug with *C. cinerea* grown on YMG medium was inoculated in the centre of a *C. cinerea* minimal medium
311 (CCMM, see Supplementary Materials) agar plate. Bacteria, taken from an overnight culture, were diluted with LB
312 using a 1:25 ratio and sub-cultured aerobically for 3 h at 37°C. Bacteria were washed once with a 0.9 % w/v sodium
313 chloride solution and resuspended in CCMM to an optical density at 600 nm (OD₆₀₀) of 2. Three times 5 μ L of the

314 bacteria suspension was placed at a distance of 3.5 cm from the centre of the agar plate. The plates were incubated
315 for 5 days at 28°C in a humid and dark environment.

316

317 **Device preparation**

318 Devices were designed in AutoCAD Mechanical 2011 (Autodesk) and used to create mylar film photolithography
319 masks (Micro Lithography Services Ltd., UK). Each master mold was manufactured using conventional
320 photolithography techniques⁶² (see Supplementary Method 6 for full details). Before use with PDMS, the masters
321 were silanised under vacuum for 2 hours with 50 µL chlorotrimethylsilane (Fluka, Germany) per master.

322

323 50 g of PDMS was prepared (per master) using a 10:1 ratio of base to curing agent (Sylgard 184, Dow Corning, USA).
324 The base and curing agent were mixed together thoroughly, degassed for 1 hour under vacuum and poured on top
325 of the master. This mixture was then cured in an oven at 70°C for >2 hours. The cured PDMS was removed from the
326 master and diced to size. Holes were punched into the PDMS at specific locations, using a 3.02 mm diameter
327 precision cutter (Syneo, USA), to form the channel inlets and outlets.

328

329 Each PDMS slab was then bonded to a glass-bottomed Petri dish (dish diameter: 35 mm; glass diameter: 23 mm;
330 glass thickness: 0.17 mm; World Precision Instruments, Inc., Germany) to close the microchannels. First, the PDMS
331 slabs (after removal of scotch tape) and Petri dishes were washed and dried (see Supplementary Method 7). Bonding
332 of PDMS to the glass-bottomed Petri dishes was achieved by activating the surfaces using a glow discharge unit
333 (EMITECH K1000X, Quorum Technologies, UK) under the following conditions: polarity, negative; cycle vacuum
334 point, 1×10^{-1} mbar; plasma current, 25 mA; coating time, 1 min). Proceeding activation, the hydrophilic surfaces were
335 brought into conformal contact with one another to form a bond and 100 µL of CCMM used to fill the microchannels
336 of each device (via capillary action). An additional 100 µL of CCMM was introduced into the glass-bottomed Petri
337 dish to maintain a humid environment upon closing the Petri dish. Devices were freshly prepared for each
338 experiment in a sterile hood and used immediately. Device operation is described in Supplementary Method 1.

339

340 **Inoculation of devices with fungus**

341 Prior to inoculation of the microfluidic devices *C. cinerea* was sub-cultured at 28°C in a dark, aerated, humid box for
342 3 days. Specifically, a section of the fungal mycelium is cut from the YMG agar plate. A section is taken from the
343 peripheral growth zone and this inoculum is placed next to the device opening, such that the mycelium is in contact

344 with the glass substrate and the growth direction of the hyphal tips is orientated towards the microchannel(s). Care
345 was taken to control the size of the agar plug inoculum to ensure consistency between experiments. The Petri dish
346 was incubated in a dark and humid environment for a period of 18 hours at 28°C to allow the hyphae to grow into
347 the microchannels.

348

349 **Live-cell imaging of hyphae**

350 A widefield fluorescence microscope, based on a Nikon Ti-U inverted microscope, was used to acquire long-term
351 time-lapse experiments and is equipped with a Prior ProScan III motorised stage (Prior Scientific, UK) and CoolSNAP
352 HQ2 camera (Photometrics, Germany). Phase contrast microscopy was performed to capture brightfield images,
353 using either x10 / 0.30 NA (numerical aperture) Plan Fluor or x20 / 0.45 NA S Plan Fluor objective lenses (Nikon,
354 Switzerland) and an exposure time of 100 ms.

355

356 Conventional epifluorescence microscopy was also performed to image hyphae from the *C. cinerea* AmutBmut dTom
357 strain and the fluorescein-containing solution. A Nikon Intensilight C-HGFI mercury lamp (Nikon, Switzerland) was
358 used as the source of excitation and an exposure time of 100 ms was implemented. The following filter sets were
359 used: TRITC and FITC HC BrightLine Basic Filtersets (AHF Analysentechnik, Germany).

360

361 Micromanager (Version 1.4.12) was used to coordinate long-term time-lapse imaging experiments. Auto-focus
362 software (Simple Auto Focus, Micromanager) was implemented to correct for drift in the z-direction, induced over
363 the long-term, multi-position time-lapse experiments. All long-term time-lapse experiments were performed in a
364 dark room, where the temperature was maintained at 20°C. The Petri dish was sealed with Parafilm to prevent
365 evaporation and remained in the dark throughout the duration of the time-lapse (other than during image
366 acquisition) to minimise the onset of fungal developmental processes.

367

368 Image montages were generated using custom software and analysed using Fiji.⁶³ To measure the growth difference
369 between the time points and the cell length of the leading hyphae in each microchannel the free hand tool and
370 measuring tool of Fiji were used.

371 **Conclusions**

372 Investigations on bacterial-fungal interactions using our microfluidic platforms provided several significant
373 advantages. They enabled fungal hyphae to be cultured in microchannels, where hyphae were constricted by the
374 channel height and were thus easily imaged. Such platforms are compatible with high-resolution microscopies
375 (phase contrast, differential interference contrast (DIC), confocal, spinning disk confocal) and therefore allow live-
376 cell imaging and long-term, time-lapse microscopy to be conducted with ease. Using the BFI device, we monitored
377 the dynamic interactions of bacteria with hyphae in real-time and with single cell resolution. The presence of several
378 parallel microchannels enabled many growing *C. cinerea* hyphae to be assayed per experiment and their response,
379 upon the introduction to bacteria, to be monitored over a period of up to 24 hours (the device architecture can
380 easily be tuned to suit the growth rate of any filamentous fungus of interest). Conversely, the response of bacteria to
381 hyphae was also elucidated. It is anticipated that the coupling of automated image processing algorithms with these
382 platforms will increase the functionality of this tool, providing further opportunities to quantify the unique
383 interactions between filamentous fungi and bacteria. We were able to subject hyphae to a variety of stimuli, in a
384 rapid and controlled manner and to monitor hyphal reaction in real-time using the fluid exchange device.

385
386 We took advantage of the simplicity of the fluidic network and introduced the bacteria into the BFI device by simple
387 pipetting. Their interaction with fungal hyphae was monitored in real-time, while the fluid exchange device utilised
388 small differences in hydrostatic pressure to drive the flow and therefore enabled an exchange of the media
389 surrounding hyphae. We note that these microfluidic platforms are simple to integrate within the microbiology
390 laboratory and can be adopted for widespread use.

391
392 As a proof of principle we used these platforms to probe the interaction of *C. cinerea* with *B. subtilis*. *B. subtilis* is
393 well known for its antagonizing effects on fungi,³⁴ however our new approach provides novel insights of this
394 interaction at the cellular level and in real-time. We observe that hyphae stop growing with the formation of
395 extracellular, cytoplasm-filled blebs after contact with the wild-strain *B. subtilis* NCIB 3610, but continue to grow in
396 the presence of the lab strain *B. subtilis* 168. Growth arrest was induced by a secreted signal because addition of
397 conditioned medium using the fluid exchange device resulted in the same fungal phenotype. Furthermore, both *B.*
398 *subtilis* strains displayed a direct cellular contact with fungal hyphae that changed over time.

399

400 The design and application of microfluidic platforms has allowed us to monitor bacterial-fungal interactions at a
401 cellular level and we observed hyphal differentiation of a mycelium and bacteria-induced blebbing of hyphal cells.
402 Studying BFIs using these microfluidic platforms can provide us with an understanding of how microorganisms use
403 their antagonistic strategies in competing environments, as well as allowing the production of antimicrobial
404 substances in time and space to be located and quantified. Moreover, the technique enables the study of dynamic
405 processes, such as quorum sensing of bacterial cells in BFIs, using promoter-reporter fusions. In combination with
406 genetic and biochemical tools, microfluidic platforms provide an optimal experimental set-up to characterise the
407 interaction of fungi with bacteria at a cellular level.

408

409 Further, it is envisaged that this technology will not only impact research involving bacterial-fungal interactions, but
410 that it will also be implemented as means to study other fungal antagonists and mutualists such as nematodes,
411 plants and other fungi.

412

413 **Acknowledgements**

414 The authors would like to thank C. Villalba for construction of plasmid pMK317, Prof. Uwe Sauer, Prof. Richard
415 Losick, Prof. Masaya Fujita and Dr. Daniel Lopez for providing *B. subtilis* strains and plasmids, Oliver Dressler and
416 Adam Sheldon for custom software design, Patrick Stöckli for 3-D illustrations and Dr. Stavros Stavrakis for
417 discussions concerning microscopy. This work was supported by ETH Research Grant ETH-34 11-2 and EMBO Grant
418 ASTF 317-2010.

Figure legends

Figure 1 | Design and operation of the bacterial-fungal interaction (BFI) device. (a) Photograph illustrating the experimental setup. A PDMS top layer, containing microchannels embossed into its surface, is bonded to a glass petri dish and the channels filled with aqueous medium. A fungal inoculum is placed next to the opening of the microchannels. Following incubation, the device can be co-inoculated with bacteria at the 'bacterial inlet'. Scale bar, 5 mm. (b) Three-dimensional representation of the PDMS top layer containing the microchannels. The entrance to the microchannels can be observed and the growth direction of the hyphae is highlighted. (c) Two-dimensional representation of the BFI device illustrating its key features: constrictions for limiting the number of hyphae entering into the device and hyphal observation channels for monitoring bacteria-fungi interactions for up to 24 h. Scale bar, 3 mm. (d) Enlarged region of the design, depicted by the red box. Scale bar, 100 μm . (e) An example of *C. cinerea* hyphae growing in the microchannels. A branching event and clamp cell formation can be observed (see Supplementary Movie 1). Scale bar, 50 μm .

Figure 2 | Design and operation of the fluid exchange device. (a) Three-dimensional and (b) two-dimensional representations of the fluid exchange device highlighting its key features. Scale bar, 3 mm. (c) An enlarged region of the design, specifically depicted by the red box in (b). A tapered observation channel and narrow constriction channel were used to manipulate the direction of fluid flow towards the outlet, providing regions of low and high resistance respectively. Fluid delivery channels were located at the entrance of the tapered observation channel to minimise blockages by growing hyphae. Scale bar, 100 μm . (d) Time-lapse of *C. cinerea* minimal medium (CCMM) exchange with a fluorescein solution using the fluid exchange device (brightfield and fluorescence channels merged). Full (100 %) exchange took place within 3-4 minutes (see Supplementary Figure S1 and S2 for control experiments). Scale bar, 50 μm . (e) Before and after removal of the fluorescein solution with CCMM. Scale bar, 50 μm .

Figure 3 | Interaction of *C. cinerea* with two different *B. subtilis* strains. (a) Confrontation assay on CCMM agar plates illustrating the different response of *C. cinerea* growth alone (top) and in presence of *B. subtilis* 168 (*Bs* 168, middle) and *B. subtilis* NCIB 3610 (*Bs* NCIB 3610, bottom). A growth inhibition zone was only observed upon co-inoculation with *B. subtilis* NCIB 3610. Scale bar, 20 mm. (b) and (c) represent exemplar data that were gained at the micro level using the BFI device. The physical interaction between the *C. cinerea* hyphae and *B. subtilis* cells was

observed. The polar attachment of bacteria to the hyphae and attachment of bacteria to certain hyphae was the same for both *B. subtilis* strains. Scale bars in **(b)** and **(c)**, 25 and 10 μm respectively.

Figure 4 | Attachment pattern of *B. subtilis* to *C. cinerea* hyphae. *B. subtilis* NCIB 3610 pMF37, expressing green fluorescent protein constitutively, and *C. cinerea* pMA412, expressing dTomato constitutively, were co-inoculated into the BFI device and attachment was monitored over time. Scale bar, 50 μm .

Figure 5 | Long-term observation of *C. cinerea* hyphal growth in absence and presence of the two *B. subtilis* strains. **(a)** The growth rate of the leading hyphae was measured in the BFI device over a 10 hour time period in three independent experiments. Error bars represent standard deviations from three independent experiments. The *B. subtilis* NCIB 3610 strain had a negative effect on the growth rate of the leading hyphae that was apparent 5 hours after co-inoculation. **(b)** Bright field images representing three different time points at the same site for each condition tested. Upon addition of *B. subtilis* NCIB 3610 some hyphae showed a thin morphology (depicted by arrows), whereas this was not observed after the addition of *B. subtilis* 168. Scale bars, 25 μm .

Figure 6 | *C. cinerea* hyphae morphology change in presence of *B. subtilis*. **(a)** A co-inoculation time-lapse experiment was conducted with a *C. cinerea* strain that expresses dTomato under the control of a constitutive promoter using the BFI device. The arrows highlight cells that have lost their cellular contents due to the presence of *B. subtilis* NCIB 3610. Timestamps indicate the time after inoculation of the device with bacteria. Scale bar, 25 μm . See also Supplementary Movie 7. **(b)** Depiction of a hypha that was intact at the 5 hour time point. One cell collapsed within the next 30 min. Blebs containing cellular content were located next to this hyphal cell. Scale bar, 25 μm . Time format, hh:mm.

Figure 7 | Effect of bacteria-cell free conditioned medium on *C. cinerea* hyphae. **(a)** Addition of cell-free conditioned medium from *B. subtilis* NCIB 3610 to *C. cinerea* hyphae expressing dTomato constitutively. After exchange of CCMM with the conditioned medium the form of the tip changed within a few minutes. This was followed by formation of blebs after eight minutes (see Supplementary Movie 8). Scale bar, 50 μm . **(b)** Enlarged view of the tip depicted in (a). After eight minutes the formation of blebs occurred. Scale bar, 25 μm . **(c)** Uniform growths of *C. cinerea* hyphae in the exchange device is depicted before the addition of surfactin in the first column. Scale bar, 100 μm . Brightfield and fluorescence channels merged for all images.

Figures

Figure 1

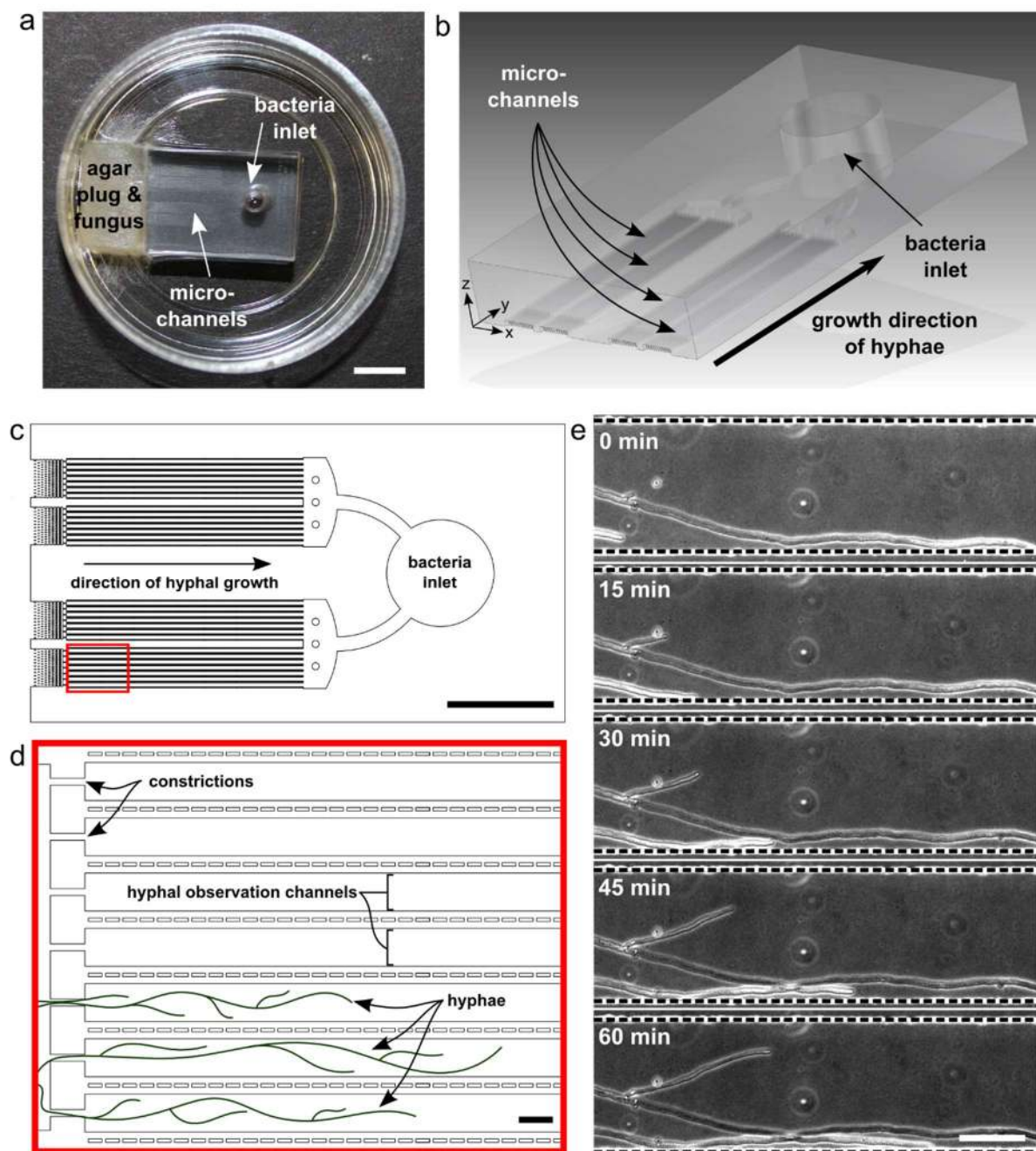


Figure 2

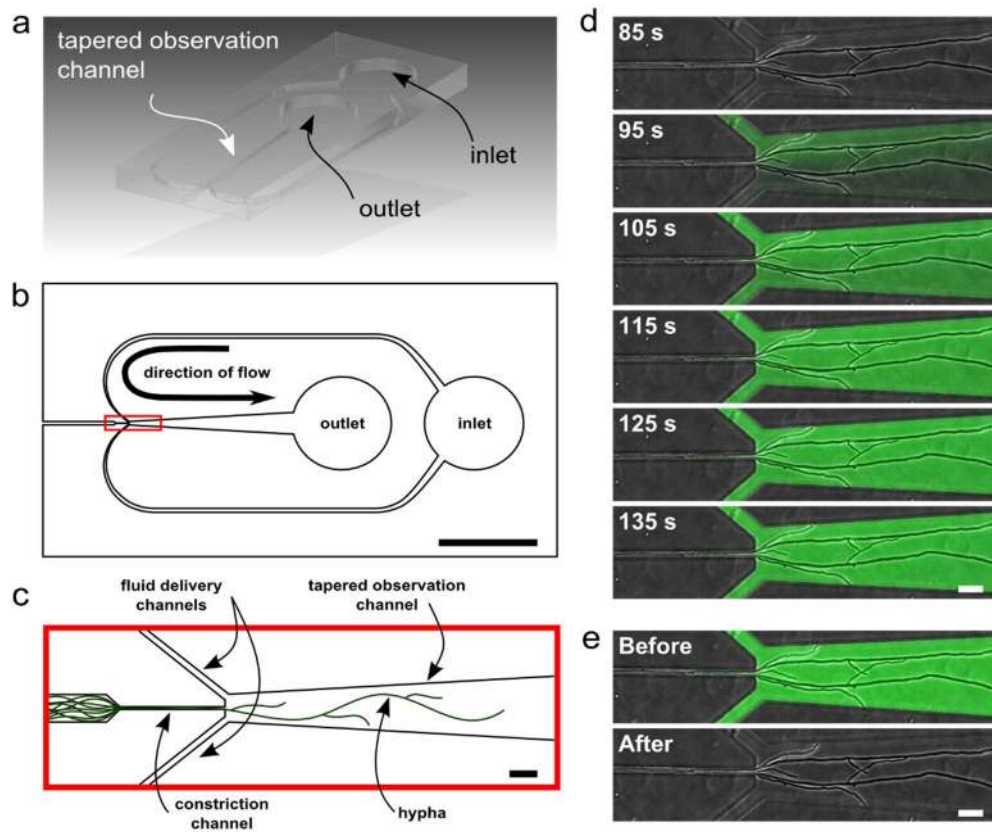


Figure 3

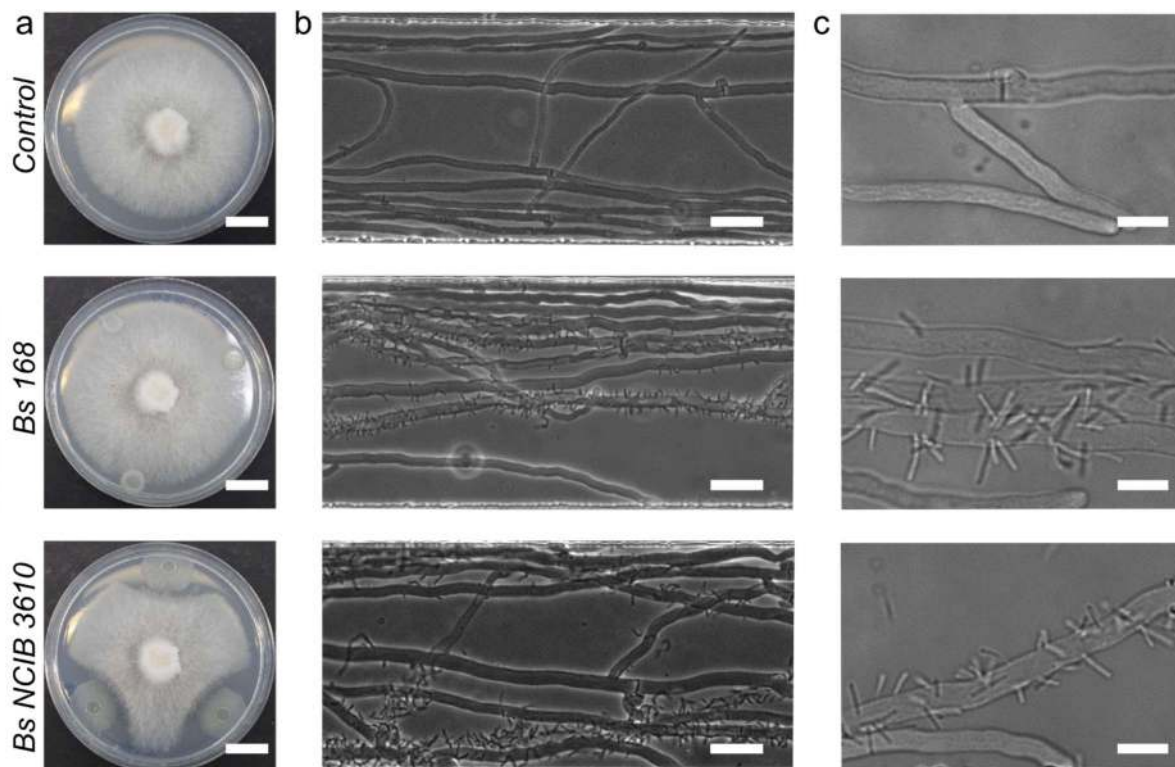


Figure 4

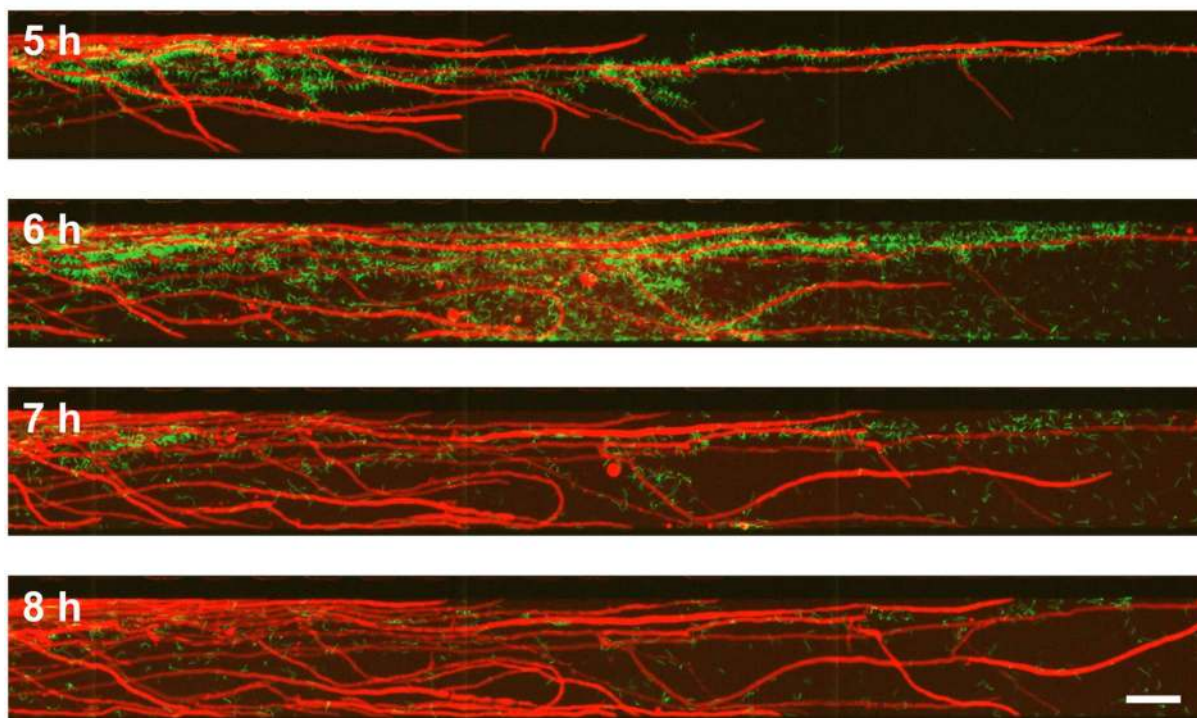


Figure 5

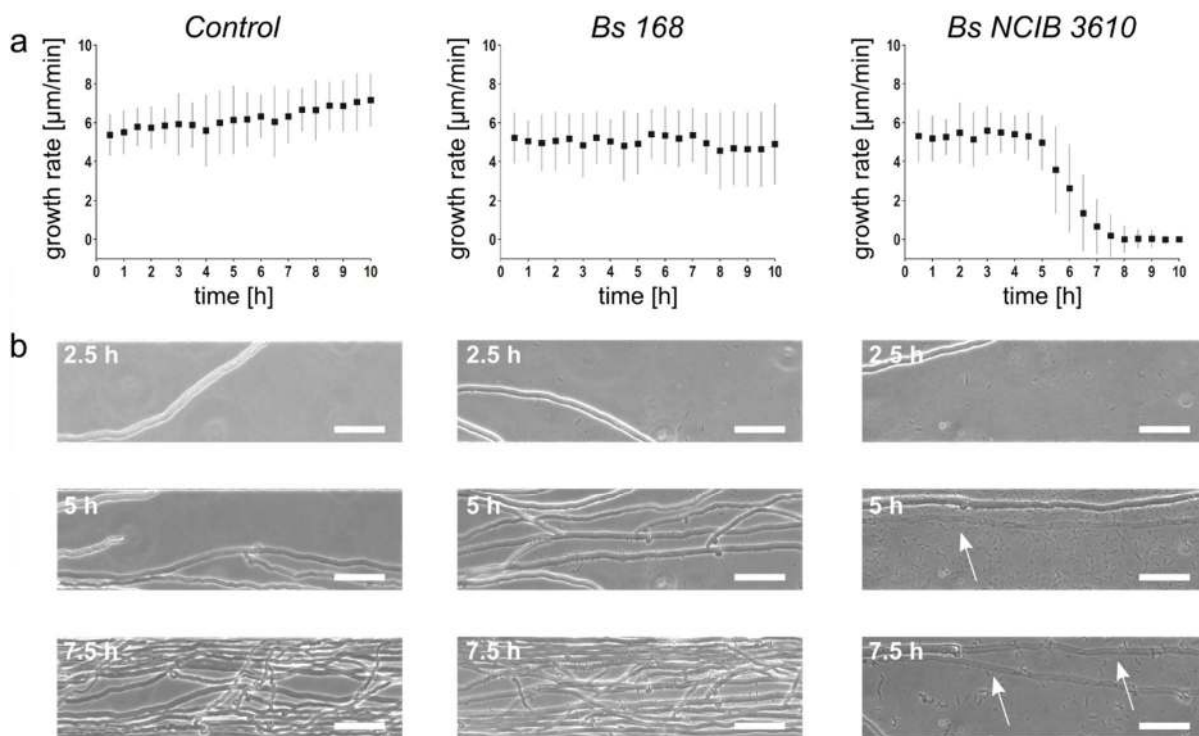


Figure 6

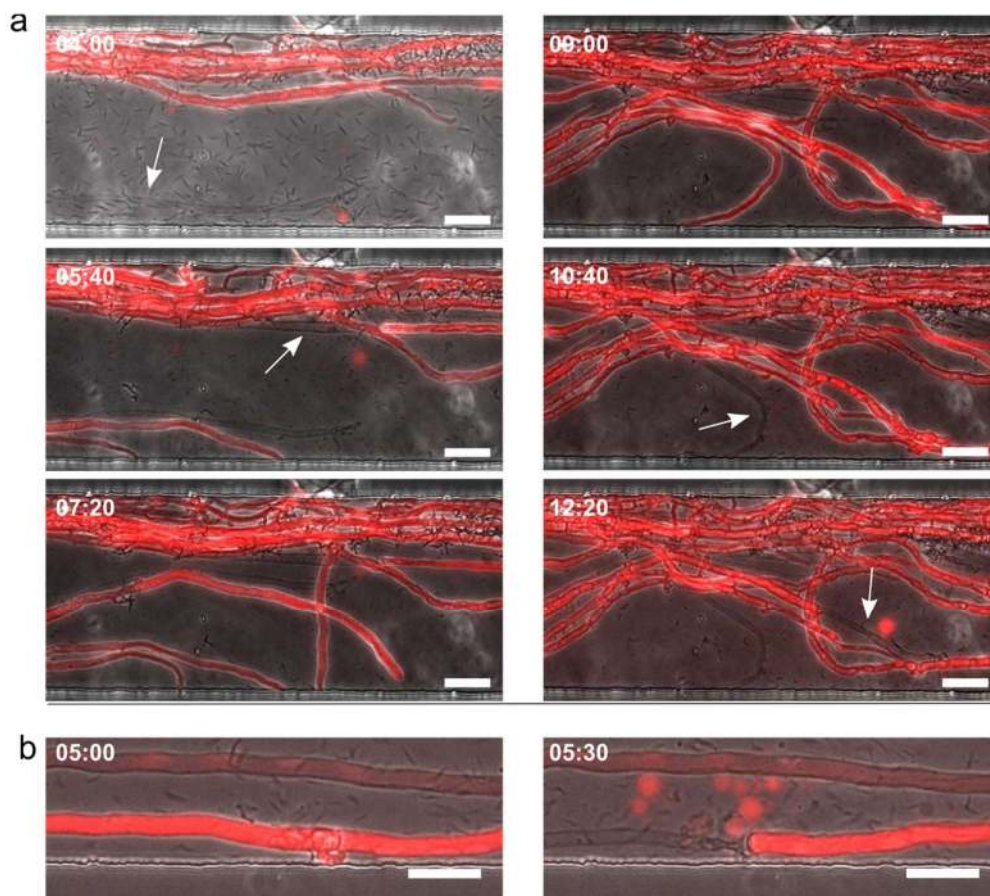
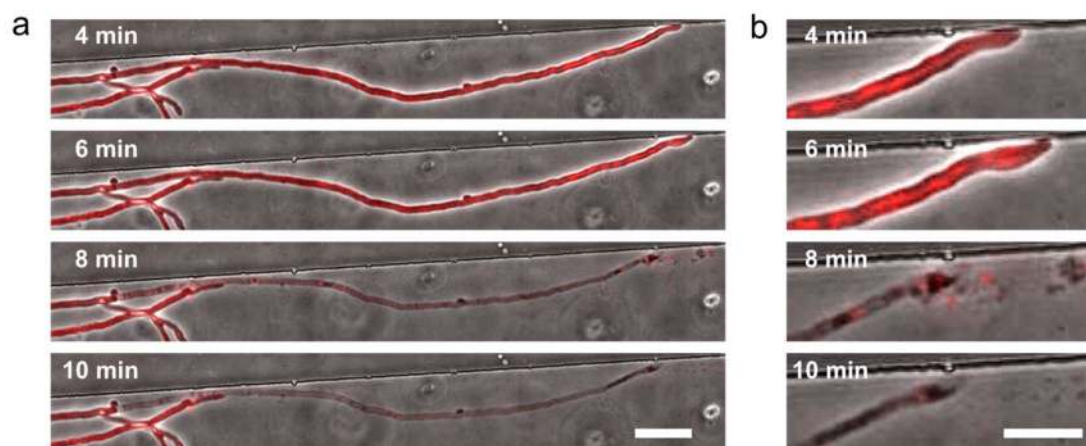


Figure 7



References

- 1 P. Frey-Klett, P. Burlinson, A. Deveau, M. Barret, M. Tarkka and A. Sarniguet, *Microbiol. Mol. Biol. Rev.*, 2011, **75**, 583-609
- 2 F. Zarenejad, B. Yakhchali and I. Rasooli, *World J. Microbiol. Biotechnol.*, 2012, **28**, 99-104
- 3 A. Deveau, B. Palin, C. Delaruelle, M. Peter, A. Kohler, J. C. Pierrat, A. Sarniguet, J. Garbaye, F. Martin and P. Frey-Klett, *New Phytol.*, 2007, **175**, 743-755
- 4 W. de Boer, L. Folman, R. Summerbell and L. Boddy, *FEMS Microbiol. Rev.*, 2005, **29**, 795-811
- 5 A. Peleg, D. Hogan and E. Mylonakis, *Nat. Rev. Microbiol.*, 2010, **8**, 340-349
- 6 B. Mogge, C. Loferer, R. Agerer, H. P. and A. Hartmann, *Mycorrhiza*, 2000, **9**, 271-278
- 7 G. F. Bills, J. B. Gloer and Z. An, *Curr. Opin. Microbiol.*, 2013, **16**, 549-565
- 8 J. Moller, M. B. Miller and A. Kjoller, *Soil Biol. Biochem.*, 1999, **31**, 367-374
- 9 A. A. Brakhage, *Nat. Rev. Microbiol.*, 2013, **11**, 21-32
- 10 T. Schneider, T. Kruse, R. Wimmer, I. Wiedemann, V. Sass, U. Pag, A. Jansen, A. K. Nielsen, P. H. Mygind, D. S. Raventós, S. Neve, B. Ravn, A. M. Bonvin, L. De Maria, A. S. Andersen, L. K. Gammelgaard, H. G. Sahl and H. H. Kristensen, *Science*, 2013, **328**, 1168-1172
- 11 H. Nützmann, Y. Reyes-Dominguez, K. Scherlach, V. Schroeckh, F. Horn, A. Gacek, J. Schümann, C. Hertweck, J. Strauss and A. Brakhage, *Proc. Natl Acad. Sci. U. S. A.*, 2011, **108**, 14282-14287
- 12 C. R. Howell and R. D. Stipanovic, *Phytopathology*, 1979, **69**, 480-482
- 13 Y. Touré, M. Ongena, P. Jacques, A. Guiro and P. Thonart, *J. Appl. Microbiol.*, 2004, **96**, 1151-1160
- 14 D. Romero, A. De Vicente, R. H. Rakotoaly, S. E. Dufour, J. W. Veening, E. Arrebola, F. M. Cazorla, O. P. Kuipers, M. Paquot and A. Perez-Garcia, *Mol. Plant Microbe Interact.*, 2007, **20**, 430-440
- 15 C. Calderón, A. de Vicente and F. Cazorla, *FEMS Microbiol. Ecol.*, 2014, DOI: 10.1111/1574-6941.12319
- 16 G. I. Souto, O. S. Correa, M. S. Montecchia, N. L. Kerber, M. Bachur and A. F. Garcia, *J. Appl. Microbiol.*, 2004, **97**, 1247-1256
- 17 G. Wichmann, J. Sun, K. Dementhon, N. L. Glass and S. E. Lindow, *Mol. Microbiol.*, 2008, **68**, 672-689
- 18 A. J. deMello, *Nature*, 2006, **442**, 394-402
- 19 F. Pereira, X. Niu and A. J. deMello, *PLoS One*, 2013, **8**, e63087
- 20 A. Fallah-Araghi, J. C. Baret, M. Ryckelynck and A. D. Griffiths, *Lab Chip*, 2012, **12**, 882-891
- 21 T. Ahmed, T. S. Shimizu and R. Stocker, *Nano Lett.*, 2010, **10**, 3379-3385
- 22 D. B. Weibel, W. R. DiLuzio and G. M. Whitesides, *Nat. Rev. Microbiol.*, 2007, **5**, 209-218
- 23 J. N. Lee, X. Jiang, D. Ryan and G. M. Whitesides, *Langmuir*, 2004, **20**, 11684-11691
- 24 J. C. McDonald and G. M. Whitesides, *Acc. Chem. Res.*, 2002, **35**, 491-499
- 25 A. K. Wessel, L. Hmelo, M. R. Parsek and M. Whiteley, *Nat. Rev. Microbiol.*, 2013, **11**, 337-348
- 26 S. Park, P. M. Wolanin, E. A. Yuzbashyan, H. Lin, N. C. Darnton, J. B. Stock, P. Silberzan and R. Austin, *Proc. Natl Acad. Sci. U. S. A.*, 2003, **100**, 13910-13915
- 27 D. Koley, M. M. Ramsey, A. J. Bard and M. Whiteley, *Proc. Natl. Acad. Sci. U. S. A.*, 2011, **108**, 19996-20001
- 28 H. Mao, P. S. Cremer and M. D. Manson, *Proc. Natl Acad. Sci. U. S. A.*, 2003, **100**, 5449-5454
- 29 J. Q. Boedicker, M. E. Vincent and R. F. Ismagilov, *Angew. Chem Int. Ed.*, 2009, **48**, 5908-5911
- 30 E. C. Carnes, D. M. Lopez, N. P. Donegan, A. Cheung, H. Gresham, G. S. Timmins and C. J. Brinker, *Nat. Chem. Biol.*, 2010, **6**, 41-45
- 31 M. Held, C. Edwards and D. V. Nicolau, *Fungal Biol.*, 2011, **115**, 493-505
- 32 J. Park, A. Kerner, M. A. Burns and X. Nina Lin, *PLoS One*, 2011, **6**, e17019

- 33 A. Essig, D. Hofmann, D. Münch, S. Gayathri, M. Kuenzler, P. T. Kallio, H.-G. Sahl, G. Wider, T. Schneider and M. Aebi, *eLife*, 2014, submitted
- 34 K. Nagorska, M. Bikowski and M. Obuchowski, *Acta Biochim. Pol.*, 2007, **54**, 495-508
- 35 U. Kües, *Microbiol Mol. Biol. Rev.*, 2000, **64**, 316-353
- 36 D. R. Zeigler, Z. Prágai, S. Rodriguez, B. Chevreux, A. Muffler, T. Albert, R. Bai, M. Wyss and J. B. Perkins, *J. Bacteriol.*, 2008, **190**, 6983-6995
- 37 Y. Chen, F. Yan, Y. Chai, H. Liu, R. Kolter, R. Losick and J. H. Guo, *Environ. Microbiol.*, 2012, **15**, 848-864
- 38 V. Leclère, R. Marti, M. Béchet, P. Fickers and P. Jacques, *Arch. Microbiol.*, 2006, **186**, 475-483
- 39 C. Burns, K. E. K. Greogory, M, M. K. Cheung, M. Riquelme, T. J. Elliott, M. P. Challen, A. Bailey and G. D. Foster, *Fungal Genet. Biol.*, 2005, **42**, 191-199
- 40 M. Fujita and R. Losick, *Mol. Microbiol.*, 2002, **43**, 27-38
- 41 A. Vinck, C. De Bekker, A. Ossin, R. A. Ohm, R. P. deVries and H. A. Wösten, *Environ. Microbiol.*, 2011, **13**, 216-225
- 42 C. de Bekker, O. Bruning, M. J. Jonker, T. M. Breit and H. A. Wösten, *Genome Biol.*, 2011, **12**, R71
- 43 A. Brand, J. D. Barnes, K. S. Mackenzie, F. C. Odds and N. A. Gow, *FEMS Microbiol. Lett.*, 2008, **287**, 48-55
- 44 J. F. Toljander, V. Artursson, L. R. Paul, J. K. Jansson and R. D. Finlay, *FEMS Microbiol. Lett.*, 2006, **254**, 34-40
- 45 V. Bianciotto, S. Andreotti, R. Balestrini, P. Bonfante and S. Perotto, *Eur. J. Histochem.*, 2001, **45**, 39-49
- 46 M. T. Brandl, M. Q. Carter, C. T. Parker, M. R. Chapman, S. Huynh and Y. Zhou, *PLoS One*, 2011, **6**, e25553
- 47 R. J. Silverman, A. H. Nobbs, M. M. Vickerman, M. E. Barbour and H. F. Jenkinson, *Infect. Immun.*, 2010, **78**, 4644-4652
- 48 J. Dijksterhuis, M. Sanders, L. G. Gorris and E. J. Smid, *J. Appl. Microbiol.*, 1999, **86**, 13-21
- 49 D. A. Hogan and R. Kolter, *Science*, 2002, **296**, 2229-2232
- 50 N. Vanittanakom, W. Loeffler, U. Koch and G. Jung, *J. Antibiot. (Tokyo)*, 1986, **39**, 888-901
- 51 R. Maget-Dana and F. Peypoux, *Toxicology*, 1994, **87**, 151-174
- 52 L. Kalai-Grami, I. Ben Slimane, M. Mnari-Hattab, S. Rezigui, M. A. Aouani, M. R. Hajlaoui and F. Limam, *World J. Microbiol. Biotechnol.*, 2013, **30**, 529-538
- 53 D. Vitullo, A. Di Pietro, A. Romano, V. Lanzotti and G. Lima, *Plant Pathol.*, 2012, **61**, 689-699
- 54 M. M. Nakano, N. B. Corbell, J and P. Zuber, *Mol. Gen. Genet.*, 1992, **232**, 313-321
- 55 D. Lopez, M. A. Fischbach, F. Chu, R. Losick and R. Kolter, *Proc. Natl Acad. Sci. U. S. A.*, 2009, **106**, 280-285
- 56 P. Zhao, C. Quan, Y. Wang and S. Fan, *J. Basic Microbiol.*, 2013, DOI: 10.1002/jobm.201200414
- 57 H. Inoue, H. Nojima and H. Okayama, *Gene* 1990, **96**, 23-28
- 58 M. A. Wälti, C. Villalba, R. M. Buser, A. Grünler, M. Aebi and M. Künzler, *Eukaryot. Cell*, 2006, **5**, 732-744
- 59 S. Swamy, I. Uno and T. Ishikawa, *J. Gen. Microbiol.*, 1984, **130**, 3219-3224
- 60 J. D. Granado, K. Kertesz-Chaloupkova, M. Aebi and U. Kües, *Mol. Gen. Genet.*, 1997, **256**, 28-36
- 61 T. J. Gryczan, S. Contente and D. Dubnau, *J. Bacteriol.*, 1978, **134**, 318-329
- 62 D. C. Duffy, J. C. McDonald, O. J. A. Schueller and G. M. Whitesides, *Anal. Chem.*, 1998, **70**, 4974-4984
- 63 J. Schindelin, I. Arganda-Carreras, E. Frise, V. Kaynig, M. Longair, T. Pietzsch, S. Preibisch, C. Rueden, S. Saalfeld, B. Schmid, J.-Y. Tinevez, D. J. White, V. Hartenstein, K. Eliceiri, P. Tomancak and A. Cardona, *Nat. Methods*, 2012, **9**, 676-682